Am J Physiol Regul Integr Comp Physiol 297: R756–R768, 2009.
First published July 9, 2009; doi:10.1152/ajpregu.00102.2009.

Correlation of cardiac performance with cellular energetic components in the oxygen-deprived turtle heart

Jonathan A. W. Stecyk,[1] Christian Bock,[2] Johannes Overgaard,[3] Tobias Wang,[3] Anthony P. Farrell,[4] and Hans-O. Pörtner[2]

[1]*Department of Zoology, University of British Columbia, Vancouver, BC, Canada;* [2]*Integrative Ecophysiology, Alfred-Wegener-Institute for Marine and Polar Research, Bremerhaven, Germany;* [3]*Zoophysiology, Department of Biological Sciences, University of Aarhus, Aarhus, Denmark; and* [4]*Department of Zoology and Faculty of Food and Land Systems, University of British Columbia, Vancouver, BC, Canada*

Submitted 13 February 2009; accepted in final form 6 July 2009

Stecyk JA, Bock C, Overgaard J, Wang T, Farrell AP, Pörtner HO. Correlation of cardiac performance with cellular energetic components in the oxygen-deprived turtle heart. *Am J Physiol Regul Integr Comp Physiol* 297: R756–R768, 2009. First published July 9, 2009; doi:10.1152/ajpregu.00102.2009.—The relationship between cardiac energy metabolism and the depression of myocardial performance during oxygen deprivation has remained enigmatic. Here, we combine in vivo ^{31}P-NMR spectroscopy and MRI to provide the first temporal profile of in vivo cardiac energetics and cardiac performance of an anoxia-tolerant vertebrate, the freshwater turtle (*Trachemys scripta*) during long-term anoxia exposure (~3 h at 21°C and 11 days at 5°C). During anoxia, phosphocreatine (PCr), unbound levels of inorganic phosphate (effective P_i^{2-}), intracellular pH (pH_i), and free energy of ATP hydrolysis (dG/dξ) exhibited asymptotic patterns of change, indicating that turtle myocardial high-energy phosphate metabolism and energetic state are reset to new, reduced steady states during long-term anoxia exposure. At 21°C, anoxia caused a reduction in pH_i from 7.40 to 7.01, a 69% decrease in PCr and a doubling of effective P_i^{2-}. ATP content remained unchanged, but the free energy of ATP hydrolysis (dG/dξ) decreased from −59.6 to −52.5 kJ/mol. Even so, none of these cellular changes correlated with the anoxic depression of cardiac performance, suggesting that autonomic cardiac regulation may override putative cellular feedback mechanisms. In contrast, during anoxia at 5°C, when autonomic cardiac control is severely blunted, the decrease of pH_i from 7.66 to 7.12, 1.9-fold increase of effective P_i^{2-}, and 6.4 kJ/mol decrease of dG/dξ from −53.8 to −47.4 kJ/mol were significantly correlated to the anoxic depression of cardiac performance. Our results provide the first evidence for a close, long-term coordination of functional cardiac changes with cellular energy status in a vertebrate, with a potential for autonomic control to override these immediate relationships.

high-energy phosphate metabolism; anoxic turtle cardiac performance; in vivo magnetic resonance spectroscopy

MOST VERTEBRATES DIE WITHIN minutes when deprived of oxygen (anoxia). This intolerance to anoxia is, at least in part, due to cardiac failure caused by the inability of anaerobic metabolism to match ATP supply to demand, leading to a decline in cardiac energy state (11). Nonetheless, while it seems obvious that perturbation of cardiac energetics contributes to the failure of an oxygen-starved heart, the exact mechanisms underlying the decline in cardiac contractile function during oxygen deprivation remain equivocal despite decades of research (1, 81). Some studies propose that depletion of high-energy phosphates [ATP and phosphocreatine (PCr)] and/or accumulation of metabolic by-products such as H^+, ADP, and inorganic phosphate (P_i) causes cardiac function to deteriorate (2, 15, 16, 22, 26, 27, 50, 63, 81). Others argue against such mechanisms (3, 14, 44, 50, 62). Moreover, the potential roles of decreased turnover of high-energy phosphate compounds (7), reduced phosphorylation potential (i.e., [ATP]/[ADP] × [P_i]) (14), and the decrease in free energy released from ATP hydrolysis (dG/dξ) (41, 42, 49) are equally ambiguous.

These contradictory conclusions have all arisen from studies using Langendorff preparations or in situ heart preparations with various mammalian species. Because cardiac energy status and performance decline precipitously within seconds to minutes in oxygen-deprived mammalian hearts, the discrepancies among studies could easily arise from the experimental difficulty associated with their short-term nature. Accordingly, to compensate for the limitations of modern measurement techniques, complex computational models have recently been developed to explain the relationship between cardiac high-energy phosphate metabolism and performance (e.g., 6, 12, 81, 84). This theoretical approach, nevertheless, only provides hypotheses and predictions for future experimental testing (81).

An alternative tactic is to take advantage of a comparative approach and study species that have evolved to tolerate prolonged anoxia. The anoxia-tolerant freshwater turtles (genera *Chrysemys*, *Chyledra,* and *Trachemys*) present an interesting animal model in this context for a number of reasons. Foremost, these reptiles are eminently amenable for long-term correlation studies of cardiac cellular energy state and function because they can survive anoxia for up to 24 h at high temperatures (20–25°C) and several months at low temperatures (3–5°C) (73). Thus, the anoxic turtle heart continues to beat and generate work, albeit at a reduced level (see subsequent paragraph), for hours to months depending on ambient temperature. This much longer time course of anoxia opens up new possibilities to correlate cardiac function and energy state.

Secondly, turtles are well suited for noninvasive in vivo NMR experiments because their anoxic cardiac performance at both warm and cold temperatures is well documented and consistent among studies (28–31, 67, 69). Briefly, a progressive, profound anoxic bradycardia reduces systemic cardiac output (Q_{sys}) and power output (PO_{sys}) by 4.5- to 20-fold to a new steady state within 1 h and ~3 days of anoxia at warm and cold temperature, respectively. Thus, anoxic turtle heart rate (f_H), Q_{sys}, and PO_{sys} are closely coordinated (29, 31, 67, 69) (see Supplemental Fig. 1 in the online version of this article). Consequently, measures of turtle f_H and Q_{sys}, which can be

Address for reprint requests and other correspondence: J. A. W. Stecyk, Dept. of Physiology, Rm. 473-HMRC, University of Alberta, Edmonton, Alberta, Canada (e-mail: jstecyk@ualberta.ca).

obtained with established in vivo MRI techniques, can be regarded as suitable proxies for other measures of cardiac performance, such as force development, contractility, and work output that cannot be measured noninvasively by MRI.

Finally, a dichotomy in autonomic cardiovascular control between warm- and cold-acclimated turtles (30, 67) renders anoxic turtles unique for an in vivo examination of a temporal relation between intrinsic cardiac performance and high-energy phosphate metabolism. At high temperatures, autonomic control of the heart is retained during anoxia exposure, with cholinergic cardiac inhibition contributing to ~36–48% of the anoxic bradycardia (30, 31). In contrast, autonomic cardiac control is severely blunted at low temperature and does not contribute to the cardiac downregulation (30). Moreover, at both high and low temperatures, other mechanisms such as α-adrenergic (69) and adenosinergic (67) inhibition are not involved in the unaccounted cardiac inhibitory mechanisms. Instead, modifications intrinsic to the heart have been implicated to contribute to the cardiac downregulation (66). Intrinsic cardiac modifications could arise easily from alteration of cardiac high-energy phosphate concentrations and, consequently, cellular energetic status. Therefore, the roles of cardiac metabolism and autonomic control in anoxic cardiac depression can be separated in vivo with investigations at both warm and cold temperatures.

High-energy phosphate metabolism of the anoxic turtle heart has been investigated previously by ^{31}P-NMR measurements on isolated, working in vitro heart preparations exposed to anoxia, acidosis, or combined anoxia and acidosis at warm temperature (37, 76, 79) and on tissues terminally sampled from 3°C turtles after 12 wk of anoxia exposure (38). Results from the in vitro studies argue against any direct causal relationship between cardiac function and high-energy phosphate compounds (ATP, PCr, and P_i) during anoxia or acidosis exposure, but they revealed that anoxia and acidosis act synergistically to depress cardiac function. However, in vitro studies depend greatly on the relevance of the in vitro extracellular conditions and cardiac performance to those in vivo. Therefore, the isolated heart preparations that were electrically paced (37) and performing at subphysiological levels (76, 79) may not create similar energetic conditions as in vivo. The terminal sampling revealed a ~40% decrease of cardiac ATP and PCr, a fall of intracellular pH (pH_i) of 0.2 units, and unchanged P_i levels (38). However, with terminal sampling, the rapidity with which tissues can be sampled from a hard-shelled animal is always a concern, and the temporal changes are undetermined. Lacking, therefore, is a clear understanding of the temporal changes in cardiac energy state that occur in vivo in warm and especially in cold turtles during anoxia.

In the present study, we provide the first continuous measurements of in vivo cardiac energetic state of an anoxia-tolerant vertebrate during prolonged anoxia. We used in vivo ^{31}P- NMR spectroscopy for direct and repeated measurements of cardiac high-energy phosphates and pH_i of unanesthetized turtles (*Trachemys scripta*) during prolonged anoxia at 21°C and 5°C. In addition, by using flow-weighted MRI techniques to monitor f_H, as well as aortic and pulmonary blood flows, we could establish a time course for changes in cardiac activity that could be directly compared with the changes in high-energy phosphates, pH_i, and energetic state of the heart.

MATERIALS AND METHODS

Experimental animals and ethical approval. Fourteen red-eared slider turtles *(T. scripta,* gray) with body masses ranging between 546 and 748 g (630 ± 76 g, means ± SD) were obtained from Lemberger (Oshkosh, WI). The seven turtles studied at 21°C were held at room temperature and a 12:12-h light-dark photoperiod for several weeks in aquaria with free access to basking platforms and water. They were fed several times a week with commercial turtle food pellets, but food was withheld for 4 days before experimentation. The other seven turtles were acclimated and studied at 5°C. These turtles had been kept in aquaria within a temperature-controlled room (5°C) for 5 wk before experimentation and had been fasted during the entire acclimation period. All experimental procedures were carried out at the Alfred-Wegener-Institute for Marine and Polar Research in accordance with German legislation.

Experimental protocol. Twenty-four hours before the in vivo MR measurements, turtles were placed individually in an enclosed, water-containing plastic chamber with access to air and were restrained by two Velcro straps glued to the bottom of the chamber to prevent large body movements and associated motion artifacts. The turtles could freely move the appendages and the head. MR measurements were carried out first under normoxic conditions and then at regular intervals during a prolonged anoxia exposure, so each animal could serve as its own control. For MR measurements during normoxia, the temperature within the magnet was set to the acclimation temperature of the animal, and the chamber containing the turtle was placed within the magnet [Bruker 47/40 Biospec DBX system with a 40-cm-wide bore and actively shielded gradient coils (50 mT/m)], and the heart was centered over a triple tuneable surface coil (^{31}P, ^{13}C, ^{1}H; 5 cm diameter) that was used for ^{31}P-NMR spectroscopy. An actively decoupled ^{1}H cylindrical birdcage resonator (20-cm diameter) was used for the MRI experiments. The coil circuit and field homogeneity were optimized to the experimental setup, and the location of the heart within the magnet was confirmed via coronal, sagittal, and transverse scout images collected using a gradient echo sequence [excitation pulse shape, hermite; pulse length, 2,000 μs, $\alpha = 22.5°$; matrix size, 128 × 128; field-of-view (FOV), 12 cm^2; slick thickness, 3 mm; repetition time (TR), 100 ms; echo time (TE), 5 ms; resulting scan time, 25 s] (see Supplemental Fig. 2 in the online version of this article). Data presented for control normoxic ^{31}P-NMR spectra and MR images were averaged from results of 4 or 5 sets of measurements that were obtained over a period of 45–60 min (see below for MR spectroscopy and imaging measurement parameters).

To create prolonged anoxia after the normoxic measurements, the chamber was filled with water of the appropriate temperature and continuously bubbled with N_2 (water $Po_2 < 0.3$ kPa). For MR measurements during anoxia, the chamber was recentered in relation to the magnet, surface coil, and resonator. For the 2.85 h anoxia exposure at 21°C, ^{31}P-NMR spectra and MR images were acquired every 10–15 min. For the 11-day anoxia exposure at 5°C, ^{31}P-NMR spectra and MR images were acquired every ~15 min for the first ~18 h and then on *days 3*, *7,* and *11* (as averages from 4 or 5 sets of ^{31}P-NMR spectra and MR images obtained over a period of 45–60 min). The duration of the anoxia exposures were similar to previous studies of cardiac control during prolonged anoxia (29, 30, 31, 66, 67, 69, 70). When not in the magnet, the 5°C anoxic turtles were returned to the cold room, and the housing chambers continuously bubbled with N_2.

^{31}P-NMR spectroscopy. In vivo ^{31}P-NMR spectroscopy parameters were as follows: sweep width, 4,000 Hz; flip angle, 60° (pulse shape, bp32; pulse length, 200 μs); TR, 1 s; scans, 512; total acquisition time, 8 min 32 s. ^{31}P-NMR spectra were processed using TopSpin v1.0 software (BrukerBioSpin MRI, Ettlingen, Germany) and an automatic analyzing routine (written by R.-M. Wittig, Alfred-Wegener-Institute for Marine and Polar Research) to yield integrals of all major peaks within the spectrum (Fig. 1), as these correlate with the amount

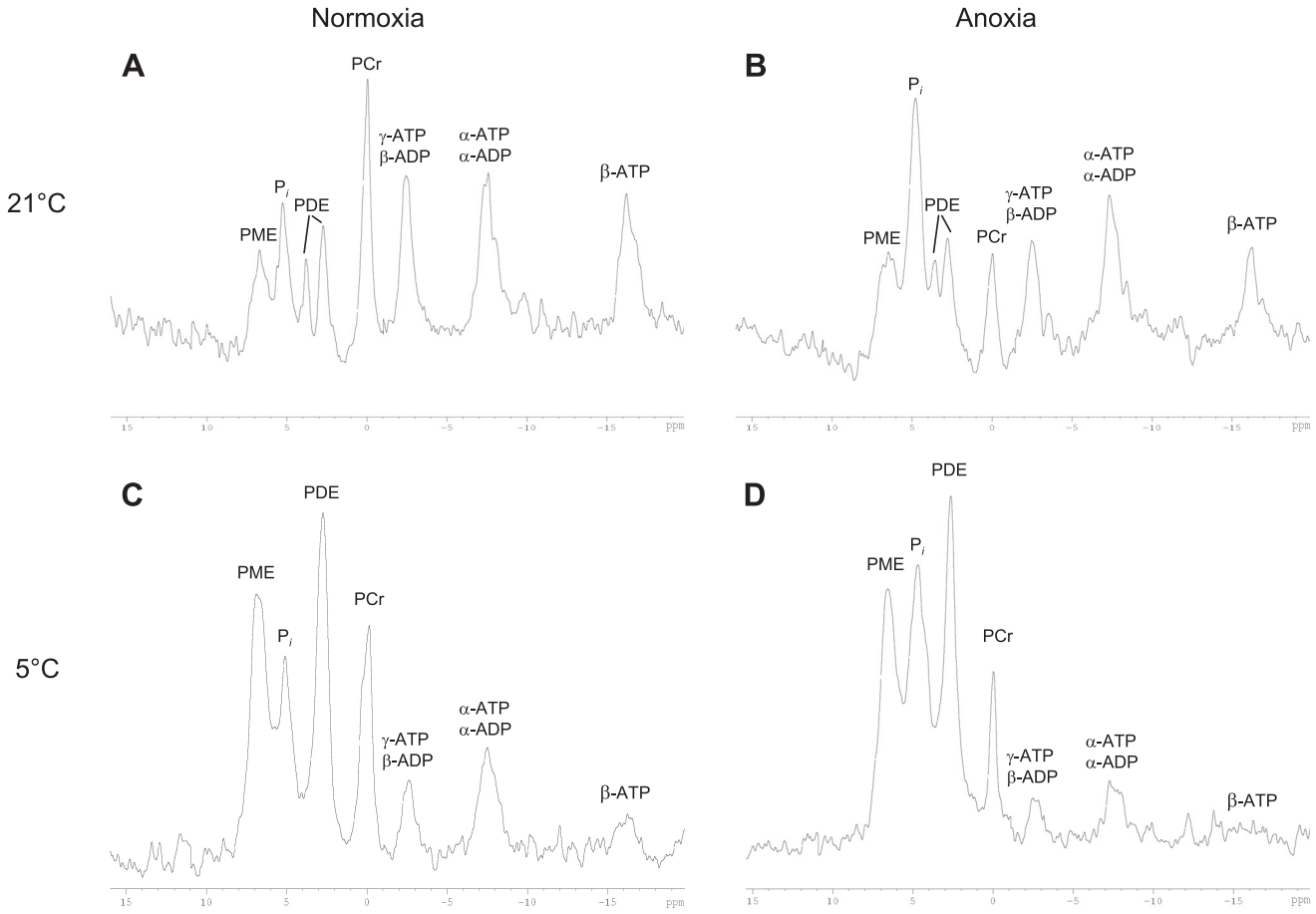

Fig. 1. Representative in vivo ^{31}P-NMR spectra of a 21°C normoxic turtle (*A*), a 21°C turtle at 2.85 h of anoxia (*B*), a 5°C normoxic turtle (*C*), and a 5°C turtle on *day 11* of anoxia exposure (*D*). PME, phosphomonoester; P_i, inorganic phosphate; PDE, phosphodiester; PCr, phosphocreatine. α-, β- and γ-ATP correspond to the three phosphates of ATP; α- and β-ADP correspond to the two phosphates of ADP.

of substance within the detection volume of the ^{31}P-NMR coil (9). Briefly, a fit function consisting of a combination of Gaussian and Lorentz line shapes (BrukerBioSpin, Ettlingen, Germany) was adjusted semiautomatically to all signals, resulting in signal integrals. This procedure allows the quantification of overlapping signals. Chemical shifts of the signals were determined using an automatic peak picking routine within the software package TopSpin v1.0 (BrukerBioSpin GmbH, Ettlingen, Germany).

MR imaging. Alternating with spectroscopy, flow-weighted MR imaging methods, previously used successfully for crustaceans and fish (8, 10, 47), were applied to measure f_H, as well as aortic and pulmonary blood flows. f_H was measured using a single slice fast gradient echo MRI sequence [Snapshot Flash (25)] with the parameters: excitation pulse shape, hermite; pulse length, 2,000 μs; flip angle, 80°; FOV, 6 cm; one axial slice, slice thickness, 2 mm; matrix, 128 × 64; TR, 8.53 ms; TE, 3.1 ms; resulting scan time, 545 ms; dummy scans, 117; repetitions, 32 for 21°C experiments, 64 for 5°C experiments; receiver gain (rg), 500. Blood flows in the left aorta and pulmonary artery were determined using the same axial view from a flow-weighted gradient echo MRI sequence similar to Bock et al. (8) with the parameters: excitation pulse shape, hermite; pulse length, 2,000 μs; flip angle, 80°; FOV, 6 cm; slice thickness, 2 mm; matrix 128 × 128 averages, 4; dummy scans, 59; rg, 1,500.

Data analysis and statistics. Concentrations of ATP, PCr, and P_i were expressed as a percentage of the total ^{31}P-NMR signal [i.e., the sum of the 7 major peaks: phosphomonoester (PME), P_i, phosphodiester (PDE), PCr, γ-ATP, α-ATP, and β-ATP; see Fig. 1] to control for *1*) possible differences in ^{31}P-NMR signal intensities that can occur from slight movement of the animal, and *2*) minor differences in the position of the turtle in the magnet before and following commencement of anoxia, as well as between measurement days. This approach assumes that no major phosphate export from turtle cardiac muscle occurs with anoxia exposure. Although no previous study has reported on the effect of anoxia on all phosphate compounds in the turtle heart, data from Jackson et al. (38) show that the sum of P_i. PCr, β-ATP, PDE, and PME does not change in anoxic 20°C-acclimated turtle hearts, but it is reduced slightly (~13%) in anoxic 3°C-acclimated hearts. Similarly, our approach was validated by observing no statistically significant changes in total ^{31}P signal during anoxia at 21°C, and a small, but insignificant 13% decrease with anoxia exposure at 5°C (see Supplemental Fig. 3 in the online version of this article). Relative metabolite concentrations were transformed to micromoles per gram quantities by setting the mean 21°C control normoxic β-ATP value to 2.9 μmol/g wet weight (38) and using this value as a conversion factor to calculate the other metabolite concentrations for both warm and cold turtles. pH_i was calculated from the chemical shift of P_i relative to PCr using previously published formulas, describing the relationship between pH and chemical shift difference for warm (76) and cold (38) turtles.

The free energy of ATP hydrolysis (dG/dξ) was estimated from pH_i and β-ATP, PCr, and P_i concentrations as described earlier (58) and is expressed as kilojoules per mole, where more negative values

indicate greater free energy available from the hydrolysis of ATP to drive ATP-requiring reactions. For the calculation of dG/dξ, molar concentrations of metabolites were calculated assuming water content of turtle cardiac tissue to be 80% (21), and levels of unbound effective P_i^{2-}, free ADP (ADP_f), and free AMP (AMP_f) were calculated on the basis of the apparent equilibrium constants of creatine kinase and adenylate kinase, which were corrected for experimental temperature and pH (48). Cytostolic [Mg^{2+}] was assumed to be 1 mM under all experimental conditions as β-ATP peak position was found not to vary significantly between acclimation temperatures or with anoxia exposure at 5°C or 21°C (data not shown). Creatine content (Cr) was estimated as the difference between the total Cr content in the turtle heart and ^{31}P-NMR measured PCr content. For 21°C turtles, total Cr is 8.14 μM/g (53). Because no previous study has reported total Cr content of 5°C turtle hearts and because PCr concentration of 5°C hearts (8.4 ± 0.5 μmol/g; Table 1) was greater than 8.14 μM/g, total creatine content was estimated to be 9.95 μmol/g at 5°C using the same ratio of Cr:PCr as for 21°C.

f_H was calculated from the time interval between Snapshot Flash MR images that depicted blood flow through the central blood vessels. Relative changes in aortic and pulmonary blood flow were determined by manually selecting regions of interest (ROIs) in the flow-weighted gradient echo MR images and comparing changes in the mean signal intensity of the ROIs. Depending on the location of the heart and quality of image, blood flow was measured from either the left or right aortic arch, as a previous study has shown blood flow through these vessels to be equivalent independent of acclimation temperature or anoxia exposure (67). Likewise, blood flow was measured from either the right or left pulmonary artery under the assumption that blood flow is equivalent in both vessels. To better compare data among turtles and compensate for potential contrast changes between images, baseline corrections were applied to individual ROIs by subtracting signal intensity of a ROI placed in a region of the image in which flow effects could be excluded (similar to Ref. 8; see Fig. 2*B*). The latter ROIs are considered as noise. In some instances, especially with prolonged anoxia at 5°C when f_H is less than 1 min^{-1}, pulmonary ROI mean signal intensity was less than the noise ROI mean signal intensity. Consequently, modest, negative values of pulmonary flow could be obtained (see Fig. 3*A*). However, because our MR imaging-determined changes in aortic and pulmonary flow closely match previous invasive measurements (see RESULTS), we interpreted the negative values as a complete cessation of pulmonary blood flow.

Statistically significant changes in measured or calculated parameters between acclimation temperatures were determined using *t*-tests. Statistically significant changes in measured or calculated parameters over time with prolonged anoxia exposure were determined using a one-way repeated-measures analysis of variance. Where appropriate, multiple comparisons were performed using Student-Newman-Keuls tests, and in all instances, significance was accepted when $P < 0.05$. All results are expressed as means ± SE.

RESULTS

Normoxia: phosphorous metabolites, pH_i and dG/dξ. Our in vivo ^{31}P-NMR spectroscopy distinguished the resonance peaks previously reported for isolated perfused turtle hearts at warm temperature (38, 76, 77) (Fig. 1). Further, our measurements of cardiac high-energy phosphate content in normoxia at 5°C and 21°C were similar to previous ^{31}P-NMR studies of isolated perfused hearts or cardiac strips from *Chrysemys picta bellii* (37, 38, 75–77, 79) as well as traditional biochemical measurements (24, 53).

We found a temperature dependence of cardiac high-energy phosphate metabolism (Table 1). Cardiac PCr, PME, PDE, ADP_f, and AMP_f content at 5°C were 1.4×, 2.7×, 2.6×, 3×, and 70× greater, respectively, than at 21°C. Similarly, normoxic pH_i, was 0.16 units greater at 5°C. In contrast, estimated dG/dξ values revealed that 5.8 kJ/mol less energy was available from the hydrolysis of ATP at 5°C. Likewise, cardiac ATP content was 48% lower at 5°C than at 21°C.

Prolonged anoxia: f_H and blood flow responses. Our MRI techniques accurately resolved f_H and central vascular blood flows, yielding similar values to those measured directly using implanted blood flow probes (29, 30, 31, 67, 69) (Figs. 3–5). Prolonged anoxia at 5°C reduced aortic blood flow by 80–90% (Figs. 2*A* and 3*A*), and f_H decreased from 4.2 ± 0.6 min^{-1} to ~1 min^{-1} (Fig. 4*A*). A steady state in f_H was reached after 3 days. A novel finding was the cessation of pulmonary blood flow with prolonged anoxia exposure at 5°C (Figs. 2*B* and 3*A*). At 21°C, anoxia reduced aortic and pulmonary blood flows by ~50% and ~85–90%, respectively (Fig. 3*B*), while f_H decreased significantly from 14.1 ± 1.7 to ~10 min^{-1} (Fig. 5*A*). A new steady state in f_H was reached after 0.42 h, after which there were no significant changes for the remainder of the ~3-h experiment.

Prolonged anoxia: phosphorous metabolite, pH_i and dG/dξ changes. Prolonged anoxia affected the myocardial phosphorous metabolite content, pH_i and dG/dξ. At 5°C, the temporal

Table 1. *Effect of temperature and anoxia exposure (2.85 h at 21°C and 11 days at 5°C) on turtle myocardial high-energy phosphate metabolism, pH_i and energetic state*

	21°C		5°C	
	Normoxia	Anoxia	Normoxia	Anoxia
ATP, μmol/g	2.9±0.3	2.4±0.2	1.5±0.2†	0.7±0.1*
PCr, μmol/g	5.8±0.9	1.8±0.3*	8.4±0.5†	3.2±0.7*
pH_i, units	7.40±0.10	7.01±0.04*	7.66±0.06†	7.12±0.04*
Total P_i, μmol/g	3.2±0.8	7.7±0.6*	4.1±0.7	8.8±0.6*
Effective P_i^{2-}, μmol/g	2.4±0.4	4.8±0.4*	3.0±0.4	5.7±0.3*
dG/dξ, kJ/mol	−59.6±1.0	−52.5±0.9*	−53.8±0.7†	−47.4±1.0*
ADP_f, μmol/g	0.02±0.004	0.03±0.003*	0.06±0.004†	0.12±0.05
AMP_f, nmol/g	0.08±0.03	0.41±0.07*	5.56±1.70†	8.36±4.94
PME,μmol/g	2.2±0.3	3.5±0.4*	6.0±0.5†	7.9±0.7*
PDE, μmol/g	3.7±0.9	3.9±0.9	9.7±0.5†	10.1±0.5

Values are expressed as means ± SE (n =7 for 21°C and 5°C Normoxia, 6 for 21°C Anoxia and 5 for 5°C Anoxia). ATP: adenosine triphosphate; PCr; phosphocreatine; pH_i: intracellular pH; P_i: inorganic phosphate; Effective P_i^{2-}: unbound P_i; dG/dξ: free energy of ATP hydrolysis; ADP_f, free adenosine diphosphate; AMP_f, free adenosine monophosphate; PME, phosphomonoester; PDE, phosphodiester. *Significant differences are $P < 0.05$ between Normoxia and Anoxia at each acclimation temperature. †Significant differences for normoxia are $P < 0.05$ between 21°C and 5°C.

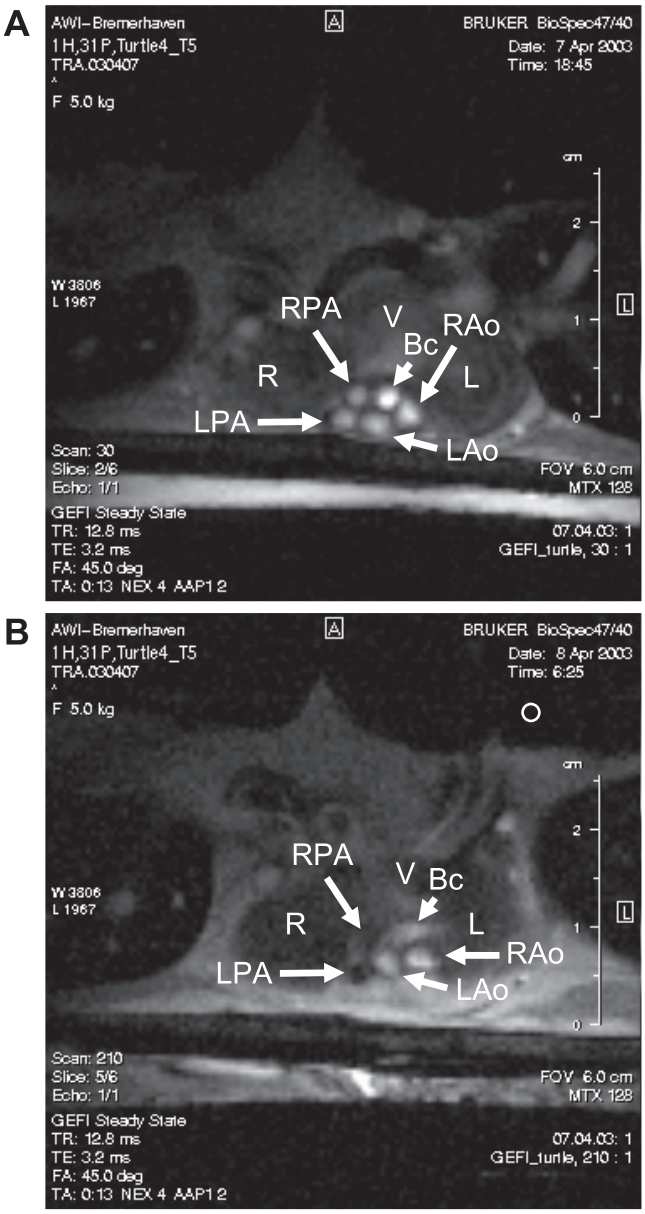

Fig. 2. Typical flow-weighted MR images of the central blood vessels of a 5°C turtle during normoxia (*A*) and following ~12 h of anoxia exposure (*B*). The magnitude of blood flow through each vessel is proportional to mean signal intensity. Note the absence of flow in the right and left pulmonary arteries and reduced blood flow in the right and left aortic arches with anoxia exposure. The open circle in the top-right corner of *B* represents the typical placement of our noise region of interest (see Supplemental Material in the online version of this article). V, ventricle; R, right atria; L; left atria, RPA, right pulmonary artery; LPA, left pulmonary artery; RAo, right aortic arch; LAo, left aortic arch; Bc; brachiocephalic artery.

change in PCr, P_i, ATP, pH_i and dG/dξ was clearly asymptotic (Fig. 4, *B–D*, *G* and *H*), suggesting that, following an initial disrupted state upon the onset of anoxia, a new steady state was established within ~3 h to 3 days (depending on the variable) of the 11-day anoxic exposure. Likewise, at 21°C, the changes in PCr, P_i, pH_i, and dG/dξ over the ~3 h of anoxia also appeared to be asymptotic (Fig. 5, *B*, *C*, *G*, and *H*), suggesting a new energetic steady state was approached within 0.9 to 1.7 h at this higher temperature. Indeed, one 21°C turtle, which was exposed to 6 h of anoxia, had clearly reached plateaus for PCr, P_i, pH_i, and dG/dξ by ~1.7 h of anoxia (Fig. 5).

After 11 days of anoxia at 5°C, PCr was reduced by 62%, total P_i was increased 2.1-fold, effective P_i^{2-} was nearly doubled, ATP was decreased by 53%, pH_i was reduced by 0.54 units, and dG/dξ was decreased by 6.4 kJ/mol (Tables 1 and 2). The respective 1.8- and 1.5-fold increases in ADP_f and AMP_f did not reach statistical significance (Fig. 4, *E* and *F*; Table 1). PME increased by 1.3-fold during anoxia, but PDE content did not change (Table 1).

After 2.85 h of anoxia at 21°C, PCr was reduced by 69%, total P_i was increased 2.4-fold, effective P_i^{2-} was doubled, pH_i was reduced by 0.39 units, and dG/dξ was decreased by 7.1 kJ/mol (Tables 1 and 2). The minor (17%) decrease in ATP was not statistically significant (Fig. 5*D*; Tables 1 and 2), but ADP_f and AMP_f increased significantly by 1.7- and 4.9-fold, respectively (Fig. 5, *E* and *F*; Table 1). Similar to 5°C turtles,

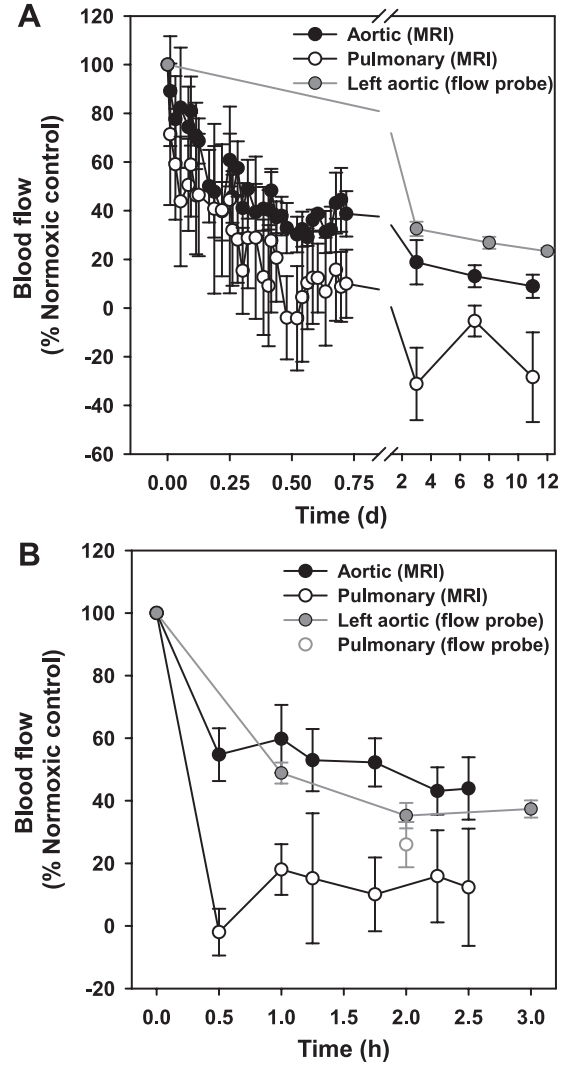

Fig. 3. Chronological changes of aortic and pulmonary blood flows in 5°C (*A*) and 21°C turtles (*B*) during prolonged anoxia exposure, as determined by MRI (present study) and by surgically implanted flow probes (data adapted from Ref. 63 for left aortic flows and Ref. 29 for pulmonary flow). Please note the different timescale between temperature acclimation groups. Values are expressed as means ± SE; n = 5–7.

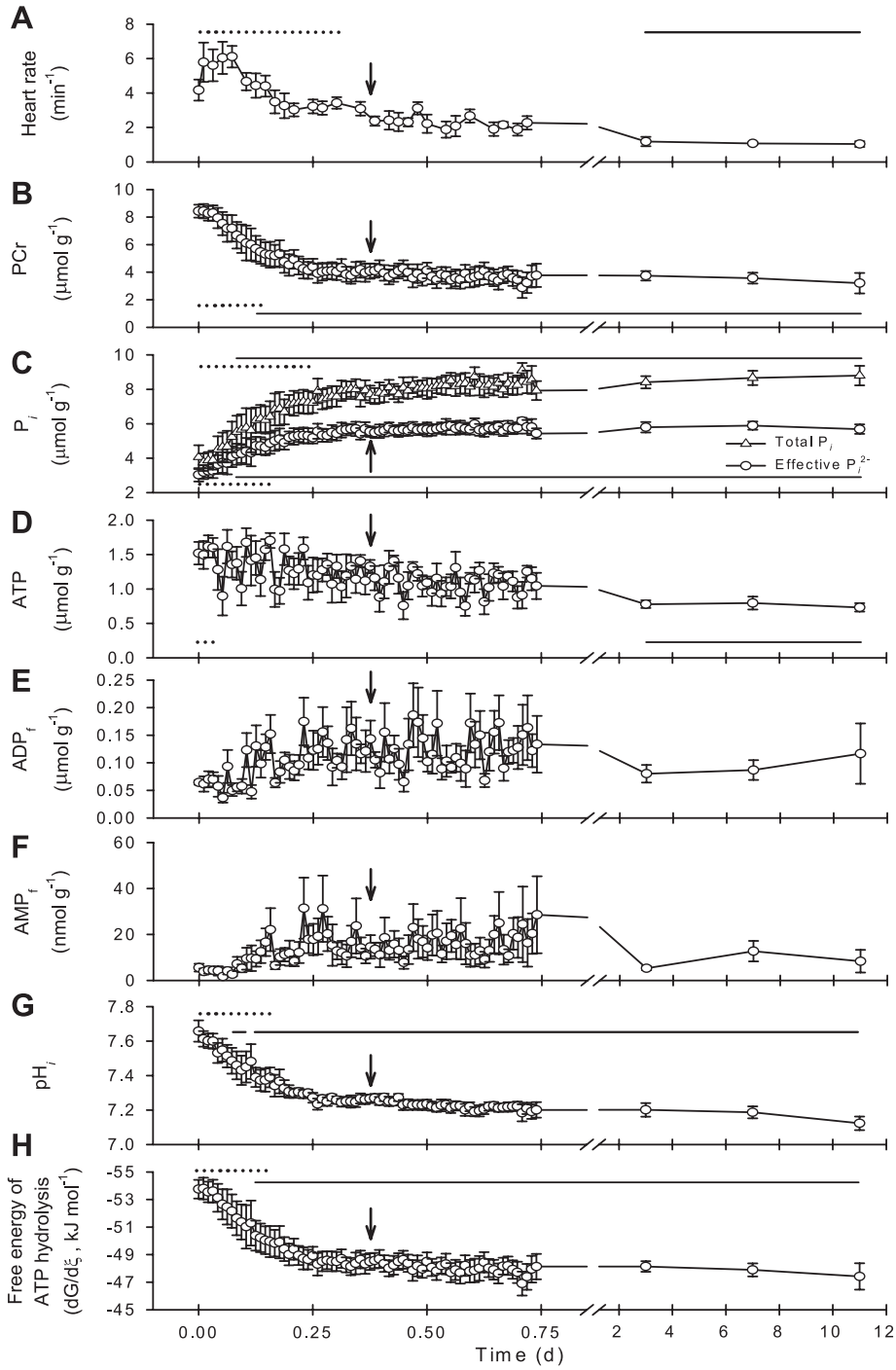

Fig. 4. Chronological changes of f_H, myocardial phosphorous metabolites (PCr; total P_i, effective P_i^{2-}; ATP, ADP_f, and AMP_f), cardiac pH_i and cardiac dG/dξ in 5°C turtles during 11 days of anoxia exposure. For each variable, statistically significant differences ($P < 0.05$) are indicated by lines above or below the traces. Solid lines indicate statistical significance from normoxic control ($t = 0$). Dotted lines indicate statistical significance from the final recording time (i.e., *day 11*). *C*: statistical significance lines for total P_i and effective P_i^{2-} are above and below the traces, respectively. Arrows indicate the anoxia exposure time temporally equivalent (assuming a Q_{10} of 2) to the 2.85-h anoxia exposure at 21°C. Values are means ± SE; $n = 5$–7.

PME increased 1.6-fold during the ~3-h anoxia exposure, but no change occurred in PDE content (Table 1).

To compare the changes in myocardial high-energy phosphate metabolism and energetic state at 5 and 21°C (Table 2), we assumed that the metabolic processes obey a Q_{10} of 2, so that the temperature difference of 16°C corresponds to a 3.2-fold difference in time. Using this approach, we found that 2.85 h of anoxia at 21°C equals 9.1 h (i.e., 0.38 day) of anoxia at 5°C (indicated by arrows in Fig. 4). This comparison revealed similar relative decreases of ATP and identical decreases of pH_i for 21°C and 5°C turtles. Even so, 21°C turtles exhibited a greater relative depletion of PCr and greater relative accumulation of both total P_i and effective P_i^{2-}. Consequently, the decrease in dG/dξ was greater at 21°C than 5°C.

Despite certain quantitative similarities in the perturbation of cardiac energy states at both temperatures, only at 5°C did the anoxic depression of cardiac activity closely reflect changes of myocardial PCr, effective P_i^{2-}, ATP, pH_i and dG/dξ (Figs. 3 and 4). Indeed, plotting 5°C anoxic f_H and aortic blood flow against changes in effective P_i^{2-}, pH_i, or dG/dξ revealed that anoxic cardiac performance was tightly matched with the changes in effective P_i^{2-}, pH_i and dG/dξ and excellent linear

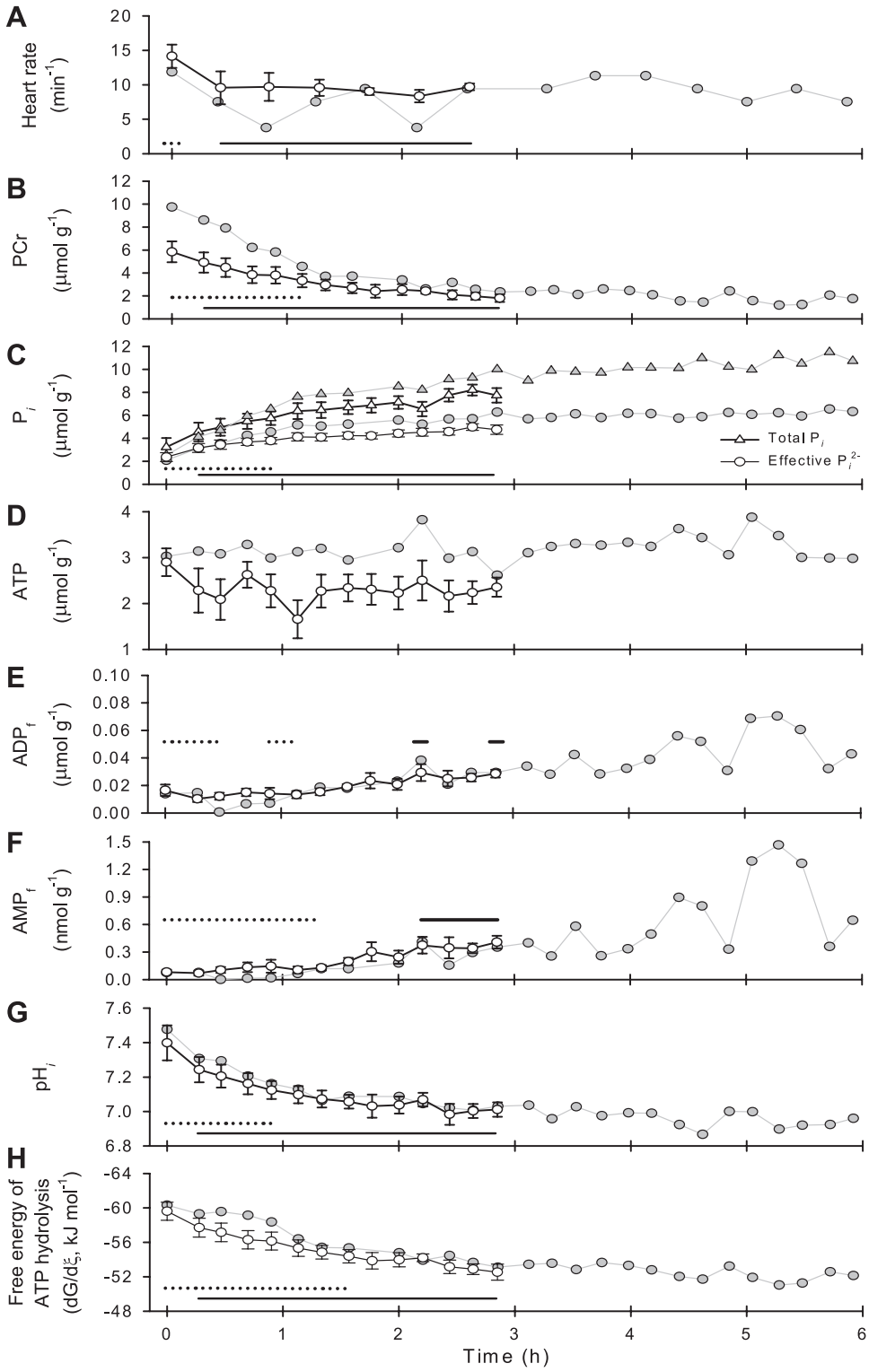

Fig. 5. Chronological changes of f_H, myocardial phosphorous metabolites (PCr; total P_i, effective P_i^{2-}; ATP, ADP_f and AMP_f), cardiac pH_i, and cardiac dG/dξ in 21°C turtles during 2.85 h of anoxia exposure. For each variable, statistically significant differences ($P < 0.05$) are indicated by lines above or below the traces. Solid lines indicate statistical significance from normoxic control ($t = 0$). Dotted lines indicate statistical significance from the final recording time (i.e., 2.85 h). *C*: statistical significance indications refer to both total P_i and effective P_i^{2-}. Open symbols are expressed as means ± SE; n = 5–7. Gray symbols are data from one turtle that was exposed to anoxia for 6 h. Values from this individual are included in the presented mean data.

regressions were obtained ($P < 0.001$; r^2 values ≥ 0.81) (Fig. 6). It should be noted that unlike for aortic blood flow (Fig. 6, *D–F*), the close coordination of f_H and cardiac energetic status was not immediately apparent with the onset of anoxia. Immediately following the commencement of anoxia, f_H of 5°C turtles increased from ~4 to ~6 min^{-1}, where it remained relatively stable until 1.7 h (Figs. 4*A*; 6, *A–C*). Concurrently, measures of cardiac energetic status either remained stable for a minimum of 15 min to a maximum of 1.7 h before showing signs of change (i.e., ATP, PCr, total P_i, dG/dξ, ADP_f, and AMP_f) or immediately changed values (i.e., pH_i, and effective P_i^{2-}) (Figs. 4 and 6). At 1.7 h of anoxia, the bradycardia typical of anoxic turtles was initiated and, near this time point, the alterations in PCr, total P_i, effective P_i^{2-}, pH_i, and dG/dξ

Table 2. *Comparison of the effect of anoxia on myocardial high-energy phosphate metabolism, pH_i, and energetic state between 21°C and 5°C turtles*

	21°C	5°C	
	2.85 h of Anoxia	9 h of Anoxia	11 Days of Anoxia
ATP	−0.17×	−0.13×	−0.53×
PCr	−0.69×	−0.51×	−0.62×
pH_i, units	−0.39	−0.39	−0.54
Total P_i	+2.4×	+1.9×	+2.1×
Effective P_i^{2-}	+2×	+1.8×	+1.9×
dG/dξ, kJ/mol	−7.1	−5.3	−6.4

Magnitudes of change were calculated between normoxic values and those at the indicated time points of anoxia exposure. Nine hours of anoxia exposure at 5°C is assumed to be temporally equivalent (assuming a Q_{10} of 2) to the 2.85 h anoxia exposure duration at 21°C (see text for details).

became significantly different from control normoxic values (Fig. 4). Thus, for f_H, 1.7 h was the initial time used in the linear regression analyses.

In contrast to 5°C turtles, f_H and aortic blood flow responses to anoxia at 21°C were not correlated with any measure of cardiac energy status (Figs. 3 and 5). Instead, f_H and aortic blood flow stabilized within 0.5 h of the commencement of anoxia, whereas PCr, P_i, pH_i, and dG/dξ continued to either increase or decrease until 0.90–1.77 h of exposure, as evidenced by the values not being statistically similar to the 2.85 h values until this time. As a result, neither f_H nor aortic blood flow was correlated with effective P_i^{2-}, pH_i, or dG/dξ (Fig. 7).

DISCUSSION

Our primary objective was to address whether decreased cardiac performance during oxygen deprivation correlates to disruptions in cardiac energy metabolism. This important basic, clinical, and pathophysiological question has been extremely difficult to study in mammals because both cardiac metabolism and power output dissipate rapidly when oxygen is unavailable. We circumvented this quandary by combining in vivo ^{31}P-NMR spectroscopy and MRI to simultaneously measure cardiac energetics and performance during prolonged anoxia with anoxia-tolerant turtles. The turtle lent itself for this study because cardiac metabolism and power output decline slowly and reach new steady states during anoxia, allowing for an excellent time resolution of biochemical and functional parameters. Moreover, the absence of autonomic cardiac control in 5°C turtles, but its presence in 21°C turtles (30, 67), enabled the roles of cardiac metabolism and autonomic control in anoxic cardiac depression to be separated in vivo. We conclude that a causal relationship exists between anoxic cardiac cellular energy status and cardiac performance when autonomic control was absent at 5°C, but not in the presence of autonomic cardiac control at 21°C.

Critique of methods. The conclusions drawn regarding the relationship between turtle cardiac energetic components and cardiac performance are based on the assumption that MRI measurements of f_H and aortic blood flow (i.e., Q_{sys}) faithfully reflect cardiac work output. We are confident of this approach because numerous previous in vivo studies have shown anoxic turtle PO_{sys} to be closely coordinated to Q_{sys} and f_H (29, 31, 67, 69) (see Supplemental Fig. 1 in the online version of this article), and our MRI techniques provided reliable f_H and aortic blood flow measurements. Specifically, our reported stable anoxic f_H of ~1 min^{-1} at 5°C and 10 min^{-1} at 21°C and the depression of aortic blood flow by 80–90% at 5°C and ~50% at 21°C are very similar to previous measurements with implanted blood flow probes (29–31, 67, 69) (Figs. 3–5). Indeed, at both acclimation temperatures, the relationship between cardiac energetic components and cardiac performance was very similar independent of whether f_H or aortic blood flow was examined, albeit for a notable distinction during the initial 1.7 h of the 11-day anoxia exposure at 5°C (Figs. 6 and 7). Considering the fact that f_H and Q_{sys} are not necessarily regulated by the same cellular mechanisms, we feel the overall consistency and redundancy in our findings add credence to the notion that changes in cardiac energetic components likely play an important role in mediating the overall depression in cardiac performance in cold, anoxic turtles.

Correlation of turtle cardiac energetic components and cardiac performance. The present study strongly suggests that alterations of effective P_i^{2-}, pH_i, and/or dG/dξ may play important roles for the depression of cardiac activity in freshwater turtles during prolonged anoxia at 5°C, but not at 21°C (Figs. 6 and 7). The disparate findings between 21°C and 5°C could reflect the different roles of the autonomic cardiac control system. At 21°C, autonomic cardiac control is an important regulator of anoxic cardiac status (30, 31). It is, thus, foreseeable that parasympathetic cholinergic cardiac inhibition decreases cardiac activity faster than the potential negative effects of cellular perturbations, whereas sympathetic adrenergic cardiac stimulation serves to maintain cardiac activity in the face of the negative effects of increased effective P_i^{2-}, reduced pH_i, and dG/dξ. For example, negative chronotropic and inotropic effects of extracellular acidosis, and the associated intracellular acidosis, on the turtle myocardium (75, 76) can be offset with adrenergic stimulation in vitro (54, 64–66, 83). In contrast, at 5°C, when autonomic cardiac control is severely blunted (30), the negative effects of cellular perturbations on cardiac performance likely predominate.

The decreased pH_i during prolonged anoxia is a potential candidate for mediating the depression of anoxic cardiac performance at 5°C. For mammalian hearts, it is well established that acidosis negatively affects cardiac chronotopy and inotropy. The negative chronotropic effects arise from the direct effect of protons on sinoatrial (60. 61) and atrioventricular node electrophysiology (13). The negative inotropic effects result from the inhibitory effect of protons on the numerous proteins involved in Ca^{2+} cycling, as well as on the sensitivity of troponin C to Ca^{2+} (reviewed by Refs. 52 and 82). For the turtle myocardium, acidosis has been shown to slow the maximum rate of force development during contraction in warm-acclimated hearts (64, 65) and reduce twitch force in cold-acclimated hearts (54). Thus, it is highly probable that decreased pH_i contributes to the anoxic cardiac downregulation at 5°C via negative inotropic effects. In contrast, other findings suggest that reduced pH_i may not be important in reducing f_H of 5°C anoxic turtles. This is because cold-acclimation appears to precondition the turtle heart and improve its chronotropic tolerance to anoxia and the accompanying acidosis (66). Specifically, spontaneous f_H of 5°C-acclimated turtles only slows during a combination of anoxia, acidosis, and hyperkalemia (66), whereas these extracellular changes, individually as well

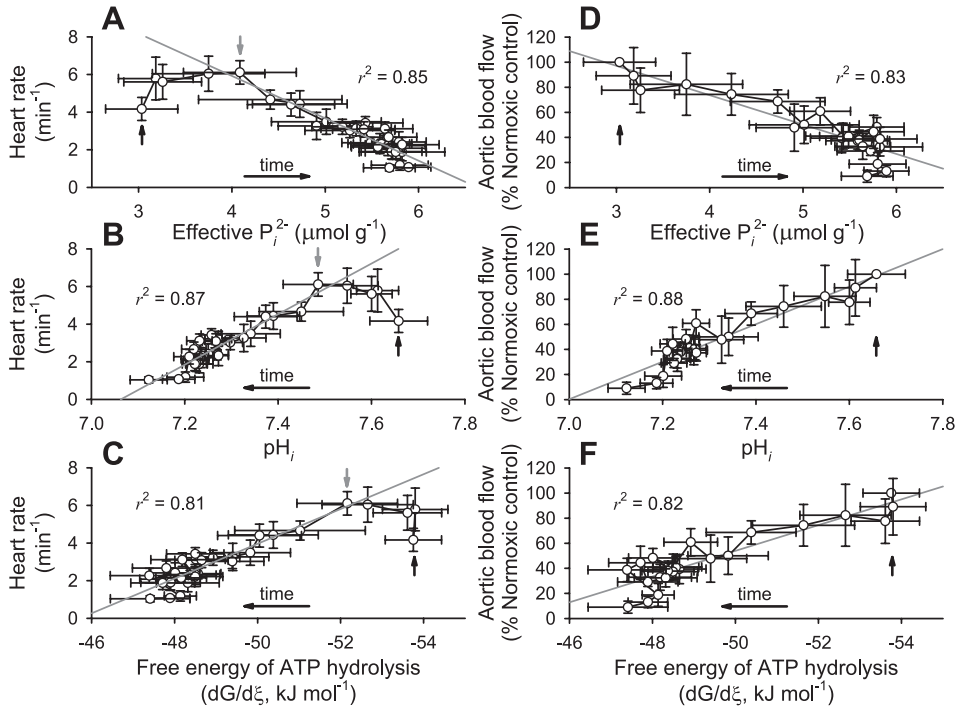

Fig. 6. Relationships between f_H (*A–C*) and aortic blood flow (*D–F*) and myocardial effective P_i^{2-} (*A*, *D*), pH_i (*B*, *E*), and dG/dξ (*C*, *F*) of 5°C turtles exposed to 11 days of anoxia. Vertical black arrows indicate control normoxic (t = 0) values. For the f_H data (*A–C*), vertical gray arrows indicate the initial time (t = 1.7 h) utilized in linear regression analyses (see RESULTS). Values are expressed as means ± SE; n = 5–7.

as collectively, do slow the spontaneous f_H of warm-acclimated hearts (18, 35, 59, 66, 75–77, 79, 83).

The elevation of unbound effective P_i^{2-} during prolonged anoxia at 5°C could also depress cardiac activity. In mammals, elevated P_i diminishes the fraction of activated actin-myosin cross-bridges, reduces the calcium sensitivity of troponin C (22, 56), and has been argued to be the major determinant of hypoxic contractile failure (6, 16, 26, 81). Likewise, contraction force and calcium sensitivity of turtle atrial tissue at high temperature decreases with increased P_i (39). However, increased ADP concentration counteracts the negative inotropic effects of P_i (39). In the present study, normoxic myocardial ADP_f was 3-fold greater at 5°C than at 21°C (Table 1). The elevated ADP_f could perhaps serve as a preparatory defense strategy to counteract the inevitable accumulation of P_i associated with the utilization of the large PCr store during winter anoxia. Furthermore, the negative effects of P_i on the turtle myocardium will also be counteracted by the intracellular acidosis that would protonate some of the accumulating P_i^{2-}.

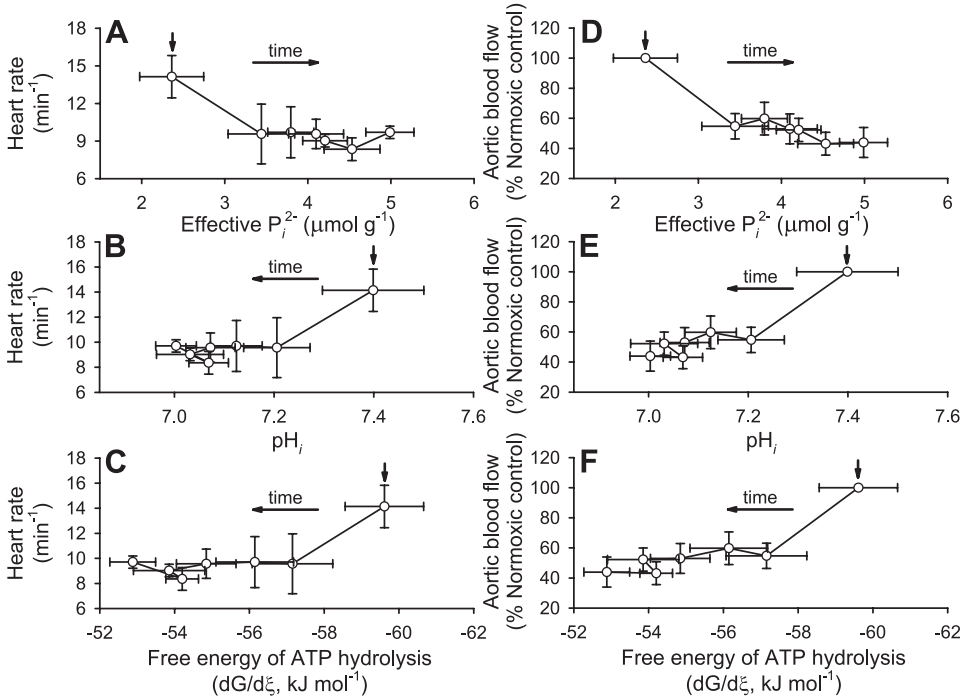

Fig. 7. Relationships between f_H (*A–C*) and aortic blood flow (*D–F*) and myocardial effective P_i^{2-} (*A*, *D*), pH_i (*B*, *E*), and dG/dξ (*C*, *F*) of 21°C turtles exposed to 2.85 h of anoxia. Vertical black arrows indicate control normoxic (t = 0) values. Values are expressed as means ± SE; n = 5–7.

The strong correlations between dG/dξ and f_H and dG/dξ aortic blood flow during prolonged anoxia at 5°C suggest dG/dξ influences cardiac performance (Fig. 6, *C* and *F*). Decreased dG/dξ is reasoned to impair cardiac activity because cardiomyocytes require a high phosphorylation potential (i.e., ratio of [ATP]/[ADP_f][P_i]), and hence, a favorable dG/dξ to drive ATPase-dependent reactions (33). Therefore, a decrease of dG/dξ below the energy level required for any particular ATP-consuming process involved in cardiac contraction and repeated action potential generation could diminish cardiac performance (40). Nonetheless, experimental support for this theory is contradictory in mammals (41, 42, 49), but it has been proposed that a reduced dG/dξ decreases cardiac performance by diminishing Ca^{2+} pumping capacity of the sarcoplasmic reticulum (SR), which ultimately leads to less Ca^{2+} that can be released from the SR to activate the contractile system upon excitation (23). A similar mechanism seems unlikely for the turtle because the SR plays a very minor role in their beat-to-beat cardiac Ca^{2+} cycling (19, 20). However, it remains to be studied whether SR Ca^{2+} cycling is enhanced at low temperature in the turtle, as in cold-acclimated fish (*Oncorhynchus mykiss*) (74). Obviously, much future work is needed to fully elucidate how decreased dG/dξ is manifested as a reduction in turtle cardiac performance.

The initial rise in f_H during the first 1.7 h of anoxia at 5°C did not correlate with key cardiac energetic components, whereas the fall in aortic blood flow was immediately correlated to changes in energetic components (Fig. 6). If f_H is viewed as the superior surrogate for cardiac work, the initial lack of correlation may be the result of a transient stress response, similar to that displayed by some ectothermic vertebrates at the onset of hypoxia exposure (5, 57), overriding the effects of changes in high-energy phosphate metabolism on cardiac performance. Alternatively, the discrepancy could indicate that the inherently different cellular mechanisms regulating cardiac chronotropy and inotropy have dissimilar sensitivities to disruptions of cellular energetic components. Specifically, our data suggest that processes involved in regulating Q_{sys} are more sensitive than those involved in regulating f_H. In this regard, it is interesting to note that turtle dG/dξ in normoxia at 21°C (−59.6 kJ/mol) and 5°C (−53.8 kJ/mol) falls below the −63.5 kJ/mol deemed critical of cardiac contraction in the mammalian heart (81). The lower dG/dξ in the turtle is less than that expected solely by the temperature difference, implying that the critical cardiac dG/dξ may vary between turtles and mammals and that the physiological processes underlying cardiac contraction of the turtle heart may operate with an inherently lower free-energy requirement. This may possibly be related to the considerably lower cardiac power output in turtle compared with mammals. On the other hand, dG/dξ of the anoxic turtle heart never dropped below the critical value of −45 kJ/mol advanced by Kammermeier et al. (41), indicating the possibility of a common anoxic critical cardiac dG/dξ among vertebrates.

Anoxic cardiac energetic status. Beyond describing the temporal relationship between cardiac high-energy phosphate metabolism and performance, the magnitude and time-course of change in myocardial high-energy phosphates, pH_i, and dG/dξ during anoxia lead to three inferences of turtle anoxic cardiac energetics.

First, anoxic turtles reorganized their cellular energetic state to a new, but lower steady state within hours, taking slightly longer at the colder temperature. This phenomenon is clearly reflected by the asymptotic change of high-energy phosphates, pH_i and dG/dξ, during the onset of anoxia and their subsequent stability (Figs. 4 and 5). Such reorganization requires that cardiac energy-consuming processes be reduced during anoxia. At the organismal level, the anoxic turtle drastically reduces ATP demand by decreasing metabolic rate (28, 34). In liver and brain, this metabolic depression involves suppression of protein turnover by "translational arrest," a reduction of transmembrane ion movement via "channel arrest" and a reduction of electrical activity of brain cells by "spike arrest" (reviewed by Refs. 32, 36, 51, 72). Anoxic depression of resting cardiac metabolic rate also contributes to decreased cardiac ATP demand (53), but the reduction in mechanical work, driven largely by anoxic bradycardia, represents the primary energy-saving mechanism (17, 29, 55, 71). Thus, in line with the depression of whole body metabolism, a 6- to 22-fold reduction in PO_{sys} lowers cardiac ATP demand well below the capacity for cardiac anaerobic ATP generation (17, 29). At the cellular level, translational arrest has been documented in the warm, anoxic turtle ventricle (4), but anoxic channel arrest does not seem to occur (70, 71). Ventricular β-adrenergic receptor density, nevertheless, is down-regulated in anoxia, rendering their heart less sensitive to adrenergic stimulation (30, 66) in spite of the very high levels of circulating catecholamines (43). In mammalian hearts, inotropic agents increase performance and counteract cardiac failure during hypoxia. However, by augmenting cardiac energetic costs, they ultimately increase, rather than decrease, heart failure mortality (33). Thus, the blunting of autonomic control in cold-acclimated turtles may be critical to conserving energy.

Secondly, our data reveal that the creatine kinase equilibrium played an important role in supplying ATP during early phases of anoxia at both temperatures. As shown previously for anoxic turtle heart and brain (38, 76, 79, 80), the reduction of PCr during anoxia was mirrored by a rise of total P_i (Figs. 4 and 5). In this regard, the higher content of PCr at 5°C in normoxia may be a preparatory response for winter hibernation. On the other hand, depletion of a large PCr store would increase P_i, which may reduce contractility (39), but, as discussed above, cold turtles appear to have strategies to counteract increased P_i^{2-} during prolonged anoxia. Likewise, the greater abundance of PME and PDE at 5°C than 21°C in normoxia (Table 1) may also be a preparatory response for winter anoxia. PDEs are greater in hearts of anoxia-tolerant turtles compared with anoxia-intolerant species, and their lysophospholipase inhibitory function has been hypothesized to be important for tolerance to anoxia and ischemia (78).

The third inference relates to important similarities and differences between temperatures. In some regard, the changes in high-energy phosphate metabolism were very similar between temperatures when a Q_{10} of 2 is taken into consideration (Table 2). ATP and pH_i, for example, were altered by identical amounts after ~3 h of anoxia at 21°C and 9 h of anoxia at 5°C. However, P_i increased, while PCr and dG/dξ decreased, faster at 21°C compared with 5°C. This situation likely arises because the turtle heart exhibits inverse thermal acclimation; a phenomenon in which physiological processes not only passively decrease with cold temperature, but are additionally

actively downregulated to further minimize ATP consumption (28). Thus, cold acclimation induces an active depression of cardiac activity that both decreases ATP demand for mechanical work (28, 29, 67, 69) and extensively modifies the electrophysiology, which may further reduce energetic costs (70). Consequently, cold-acclimated turtle hearts are apparently primed to function under low energy conditions, which may translate to smaller reductions of PCr and dG/dξ and lesser accumulation of P_i at 5°C. Despite this cold-induced metabolic preparation, cardiac ATP was reset to 50% of the normoxic value by the 3rd day of anoxia at 5°C and remained at this level for a further 8 days (Fig. 4*H*). This finding clearly signifies that cardiac ATP does not have to be maintained at control normoxic levels for successful and prolonged anoxia survival.

Perspectives and Significance

In 1929, the Danish physiologist and Nobel laureate August Krogh wrote, "For such a large number of problems, there will be some animal of choice or a few such animals on which it can be most conveniently studied" (45). Here, we affirm Krogh's principle. By combining comparative physiology with modern in vivo ^{31}P-NMR spectroscopy and MRI measurement techniques, we have provided the first in vivo evidence for a close, long-term coordination of cardiac function with high-energy phosphate metabolism during an extended period of oxygen deprivation in a vertebrate. By comparison, decades of investigation of oxygen-starved mammalian hearts have not unequivocally demonstrated such a correlation. Further, we discovered that although turtle cardiac energetic status is initially disrupted with the onset of anoxia, energetic status is relatively rapidly reset to a new, reduced steady state during prolonged anoxia exposure at both high and low temperature. Again, the detection of such a phenomenon was only possible because of our choice of study species. Combined, these findings stress the worthiness of the comparative approach to important physiological questions of basic and biomedical importance. Anoxia-related diseases such as stroke and heart infarction are major causes of death, and invaluable insights could be gained by deciphering how the champions of vertebrate anoxia tolerance (i.e., the freshwater turtle and the crucian carp, *Carassius carassius*, which possess the unique ability to retain normal cardiac performance during prolonged anoxia; 68) have solved the problem of living long term without oxygen. Further, the role of autonomic control clearly needs to be investigated in whether it overrides the relationship between cellular energy status and cellular performance in mammals in similar ways as it does in turtles. Future examination is also needed to determine whether the correlation between cardiac performance and energetic status persists upon reoxygenation.

ACKNOWLEDGMENTS

This research was supported by Natural Sciences and Engineering Research Council of Canada grants to A. P. Farrell and J. A. W. Stecyk, a Company of Biologists Travel Fund, and the *Journal of Experimental Biology* Traveling Fellowship to J. A. W. Stecyk, a Response of Higher Life to Change grant (within MARCOPOLI) to H.-O. Pörtner, and Danish Research Council funding to T. Wang. Special thanks to Rolf Wittig for his postprocessing of ^{31}P-NMR spectra and flow-weighted images.

Present address of Jonathan A. W. Stecyk: Physiology Programme, Department of Molecular Biosciences, University of Oslo, P.O. Box 1041, NO-0316 Oslo Norway.

REFERENCES

1. **Allen DG, Orchard CH.** Myocardial contractile function during ischemia and hypoxia. *Circ Res* 60: 153–168, 1987.
2. **Arai AE, Pantely GA, Thoma WJ, Anselone CG, Bristow JD.** Energy metabolism and contractile function after 15 beats of moderate myocardial ischemia. *Circ Res* 70: 1137–1145, 1992.
3. **Askenasy N.** Sensitivity of mechanical and metabolic functions to changes in coronary perfusion: A metabolic basis of perfusion-contraction coupling. *J Mol Cell Cardiol* 32: 791–803, 2000.
4. **Bailey JR, Driedzic WR.** Decreased total ventricular and mitochondrial protein synthesis during extended anoxia in the heart. *Am J Physiol Regul Integr Comp Physiol* 271: R1660–R1667, 1996.
5. **Beamish FWH.** Respiration of fishes with special emphasis on standard oxygen consumption. III. Influence of oxygen. *Can J Zool* 42: 355–366, 1964.
6. **Beard DA.** Modeling of oxygen transport and cellular energetics explains observations on in vivo cardiac energy metabolism. *PLoS Compt Biol* 2: e107, 2006.
7. **Bittl JA, Balschi JA, Ingwall JS.** Contractile failure and high-energy phosphate turnover during hypoxia: ^{31}P-NMR surface coil studies in living rat. *Circ Res* 60: 871–878, 1987.
8. **Bock C, Frederich M, Wittig RM, Pörtner HO.** Simultaneous observations of haemolymph flow and ventilation in marine spider crabs at different temperatures: a flow weighted MRI study. *Magn Reson Imaging* 19: 1113–1124, 2001.
9. **Bock C, Sartoris FJ, Wittig RM, Pörtner HO.** Temperature dependent pH regulation in stenothermal Antarctic and eurythermal temperate eelpout (*Zoarcidae*): an in vivo NMR study. *Polar Biol* 24: 869–874, 2001.
10. **Bock C, Sartoris FJ, Pörtner HO.** In vivo MR spectroscopy and MR imaging on non-anaesthetized marine fish: techniques and first results. *Magn Reson Imaging* 20: 165–172, 2002.
11. **Boutilier RG.** Mechanisms of cell survival in hypoxia and hypothermia. *J Exp Biol* 204: 3171–3181, 2001.
12. **Chen F, Clarke K, Vaughan-Jones R, Noble D.** Modeling of internal pH, ion concentration, and bioenergetic changes during myocardial ischemia. *Adv Exp Med Biol* 430: 281–290, 1997.
13. **Cheng H, Smith GL, Orchard CH, Hancox JC.** Acidosis inhibits spontaneous activity and membrane currents in myocytes isolated from the rabbit atrioventricular node. *J Mol Cell Cardiol* 46:75–85, 2009.
14. **Clarke K, O'Connor AJ, Willis RJ.** Temporal relation between energy metabolism and myocardial function during ischemia and reperfusion. *Am J Physiol Heart Circ Physiol* 253: H412–H421, 1987.
15. **Eisner DA, Elliott AC, Smith GL.** The contribution of intracellular acidosis to the decline of developed pressure in ferret hearts exposed to cyanide. *J Physiol* 391: 99–108, 1987.
16. **Elliott AC, Smith GL, Eisner DA, Allen DG.** Metabolic changes during ischaemia and their role in contractile failure in isolated ferret hearts. *J Physiol* 454: 467–490, 1992.
17. **Farrell AP, Stecyk JAW.** The heart as a working model to explore themes and strategies for anoxic survival in ectothermic vertebrates. *Comp Biochem Physiol A* 147: 300–312, 2007.
18. **Farrell AP, Franklin CE, Arthur PG, Thorarensen H, Cousins KL.** Mechanical performance of an in situ perfused heart from the turtle *Chrysemys scripta* during normoxia and anoxia at 5°C and 15°C. *J Exp Biol* 191: 207–229, 1994.
19. **Galli GLJ, Gesser H, Taylor EW, Shiels HA, Wang T.** The role of the sarcoplasmic reticulum in the generation of high heart rates and blood pressures in reptiles. *J Exp Biol* 209: 1956–1963, 2006.
20. **Galli GLJ, Taylor EW, Shiels HA.** Calcium flux in turtle ventricular myocytes. *Am J Physiol Regul Integr Comp Physiol* 291: R1781–R1789, 2006.
21. **Gesser H, Jørgensen E.** pH_i, contractility and Ca-balance under hypercapnic adicosis in the myocardium of different vertebrate species. *J Exp Biol* 96: 405–412, 1982.
22. **Godt RE, Nosek TM.** Changes of intracellular milieu with fatigue or hypoxia depress contraction of skinned rabbit skeletal and cardiac muscle. *J Physiol* 412: 155–180, 1989.
23. **Griese M, Perlitz V, Jungling E, Kammermeier H.** Myocardial performance and free energy of ATP-hydrolysis in isolated rate hearts during graded hypoxia, reoxygenation and high K_e^+-perfusion. *J Mol Cell Cardiol* 20: 1189–1201, 1988.

24. **Hartmund T, Gesser H.** Cardiac force and high-energy phosphates under metabolic inhibition in four ectothermic vertebrates. *Am J Physiol Regul Integr Comp Physiol* 271: R946–R954, 1996.
25. **Hasse A.** Snapshot FLASH MRI: Applications to T1, T2, and chemical-shift imaging. *Magn Reson Med* 13: 77–89, 1990.
26. **He MX, Wang S, Downey HF.** Correlation between myocardial contractile force and cytosolic inorganic phosphate during early ischemia. *Am J Physiol Heart Circ Physiol* 272: H1333–H1341, 1997.
27. **Hearse DJ.** Oxygen deprivation and early myocardial contractile failure: a reassessment of the possible role of adenosine triphosphate. *Am J Cardiol* 44: 1115–1121, 1979.
28. **Herbert CV, Jackson DC.** Temperature effects on the responses to prolonged submergence in the turtle *Chrysemys picta bellii*. II. Metabolic rate, blood acid-base and ionic changes and cardiovascular function in aerated and anoxic water. *Physiol Zool* 58: 670–681, 1985.
29. **Hicks JMT, Farrell AP.** The cardiovascular responses of the red-eared slider (*Trachemys scripta*) acclimated to either 22 or 5°C. I. Effects of anoxia exposure on in vivo cardiac performance. *J Exp Biol* 203: 3765–3774, 2000.
30. **Hicks JMT, Farrell AP.** The cardiovascular responses of the red-eared slider (*Trachemys scripta*) acclimated to either 22 or 5°C. II Effects of anoxia on adrenergic and cholinergic control. *J Exp Biol* 203: 3775–3784, 2000.
31. **Hicks JW, Wang T.** Cardiovascular regulation during anoxia in the turtle: An in vivo study. *Physiol Zool* 71: 1–14, 1998.
32. **Hochachka PW, Buck LT, Doll CJ, Land SC.** Unifying theory of hypoxia tolerance: Molecular/metabolic defense and rescue mechanisms for surviving oxygen lack. *Proc Natl Acad Sci USA* 93: 9493–9498, 1996.
33. **Ingwall JS, Weiss RG.** Is the failing heart energy starved? On using chemical energy to support cardiac function. *Circ Res* 95: 135–145, 2004.
34. **Jackson DC.** Metabolic depression and oxygen depletion in the diving turtle. *J Appl Physiol* 24: 503–509, 1968.
35. **Jackson DC.** Cardiovascular function in turtles during anoxia and acidosis: In vivo and in vitro studies. *Am Zool* 27: 49–56, 1987.
36. **Jackson DC.** Living without oxygen: lessons from the freshwater turtle. *Comp Biochem Physiol A* 125: 299–315, 2000.
37. **Jackson DC, Shi H, Singer JH, Hamm PH, Lawler RG.** Effects of input pressure on in vitro turtle heart during anoxia and acidosis: a ^{31}P-NMR study. *Am J Physiol Regul Integr Comp Physiol* 268: R683–R689, 1995.
38. **Jackson DC, Warburton SJ, Meinertz EA, Lawler RG, Wasser JS.** The effect of prolonged anoxia at 3°C on tissue high energy phosphates and phosphodiesters in turtles: A ^{31}P-NMR study. *J Comp Physiol [B]* 165: 77–84, 1995.
39. **Jensen MA, Gesser H.** Influence of inorganic phosphate and energy state on force in skinned cardiac muscle from freshwater turtle and rainbow trout. *J Comp Physiol [B]* 169: 439–444, 1999.
40. **Kammermeier H.** High-energy phosphate of the myocardium: Concentration versus free energy change. *Basic Res Cardiol* 82 *Suppl* 2: 31–36, 1987.
41. **Kammermeier H, Schmidt P, Jüngling E.** Free energy change of ATP-hydrolysis: A casual factor of early hypoxic failure of the myocardium? *J Mol Cell Cardiol* 14: 267–277, 1982.
42. **Kentish JC, Allen DG.** Is force production in the myocardium directly dependent upon the free energy change of ATP hydrolysis? *J Mol Cell Cardiol* 18: 879–882, 1986.
43. **Keiver KM, Weinberg J, Hochachka PW.** Roles of catecholamines and corticosterone during anoxia and recovery at 5°C in turtles. *Am J Physiol Regul Integr Comp Physiol* 263: R770–R774, 1992.
44. **Koretsune Y, Corretti MC, Kusuoka H, Marban E.** Mechanism of early ischemic contractile failure. Inexcitability, metabolite accumulation, or vascular collapse. *Circ Res* 68: 255–262, 1991.
45. **Krogh A.** The progress of physiology. *Am J Physiol* 90: 243, 1929.
46. **Kübler W, Katz AM.** Mechanism of early "pump" failure of the ischemic heart: Possible role of adenosine triphosphate depletion and inorganic phosphate accumulation. *Am J Cardiol* 40: 467–471, 1977.
47. **Lannig G, Bock C, Sartoris FJ, Pörtner HO.** Oxygen limitation of thermal tolerance in cod, *Gadus morhua* L., studied by magnetic resonance imaging and on-line venous oxygen monitoring. *Am J Physiol Regul Integr Comp Physiol* 287: R902–R910, 2004.
48. **Lawson JWR, Veech RL.** Effects of pH and free Mg^{2+} on the K_{eq} of the creatine kinase reaction and other phosphate hydrolyses and phosphate transfer reactions. *J Biol Chem* 254: 6528–6537, 1979.
49. **Matthews PW, Taylor DG, Radda GK.** Biochemical mechanisms of acute contractile failure in the hypoxic rat heart. *Cardiovasc Res* 20: 13–19, 1986.
50. **Miller DD, Salinas F, Walsh RA.** Simultaneous cardiac mechanics and phosphorus-31 NMR spectroscopy during global myocardial ischemia and reperfusion in the intact dog. *Magn Reson Med* 17: 41–52, 1991.
51. **Nilsson GE, Lutz PL.** Anoxia tolerant brains. *J Cereb Blood Flow Metab* 24: 475–486, 2004.
52. **Orchard CH, Kentish JC.** Effects of changes of pH on the contractile function of cardiac muscle. *Am J Physiol Cell Physiol* 258: C967–C981, 1990.
53. **Overgaard J, Gesser H.** Force development, energy state and ATP production of cardiac muscle from turtles and trout during normoxia and severe hypoxia. *J Exp Biol* 207: 1915–1924, 2004.
54. **Overgaard J, Wang T, Nielsen OB, Gesser H.** Extracellular determinants of cardiac contractility in the cold anoxic turtle. *Physiol Biochem Zool* 78: 976–995, 2005.
55. **Overgaard J, Gesser H, Wang T.** Tribute to P. L. Lutz: cardiac performance and cardiovascular regulation during anoxia/hypoxia in freshwater turtles. *J Exp Biol* 210: 1687–1699, 2007.
56. **Palmer S, Kentish JC.** The role of troponin C in modulating the Ca sensitivity of mammalian skinned cardiac and skeletal muscle fibres. *J Physiol* 480: 45–60, 1994.
57. **Pörtner HO, MacLatchy LM, Toews DP.** Metabolic responses of the toad *Bufo marinus* to environmental hypoxia: an analysis of the critical P_{O_2}. *Physiol Zool* 64: 836–849, 1991.
58. **Pörtner HO, Finke E, Lee PG.** Metabolic and energy correlates of intracellular pH in progressive fatigue of squid (*L. brevis)* mantle muscle. *Am J Physiol Regul Integr Comp Physiol* 271: R1403–R1414, 1996.
59. **Reeves RB.** Energy cost of work in aerobic and anaerobic turtle heart muscle. *Am J Physiol* 205: 17–22, 1963.
60. **Satoh H, Hashimoto K.** Effect of pH on the sino-atrial node cells and atrial muscle of dog. *Arch Int Pharmacodyn Ther* 261: 67–78, 1983.
61. **Satoh H, Seyama I.** On the mechanism by which changes in extracellular pH affect the electrical activity of the rabbit sino-atrial node. *J Physiol* 381: 181–191, 1986.
62. **Saupe KW, Eberli FR, Ingwall JS, Apstein CS.** Hypoperfusion-induced contractile failure does not require changes in cardiac energetics. *Am J Physiol Heart Circ Physiol* 276: H1715–H1723, 1999.
63. **Schwartz GG, Schaefer S, Meyerhoff DJ, Gober J, Fochler P, Massie B, Weiner MW.** Dynamic relation between myocardial contractility and energy metabolism during and following brief coronary occlusion in the pig. *Circ Res* 67: 490–500, 1990.
64. **Shi H, Jackson DC.** Effects of anoxia, acidosis and temperature on the contractile properties of turtle cardiac muscle strips. *J Exp Biol* 200: 1965–1973, 1997.
65. **Shi H, Hamm PH, Lawler RG, Jackson DC.** Different effects of simple anoxic lactic acidosis and simulated in vivo anoxic acidosis on turtle heart. *Comp Biochem Physiol A* 122: 173–180, 1999.
66. **Stecyk JAW, Farrell AP.** Effects of extracellular changes on spontaneous heart rate of normoxia- and anoxia-acclimated turtles (*Trachemys scripta*). *J Exp Biol* 210: 421–431, 2007.
67. **Stecyk JAW, Overgaard J, Farrell AP, Wang T.** α-Adrenergic regulation of systemic peripheral resistance and blood flow distribution in the turtle (*Trachemys scripta*) during anoxic submergence at 5°C and 21°C. *J Exp Biol* 207: 269–283, 2004.
68. **Stecyk JAW, Stensløkken KO, Farrell AP, Nilsson GE.** Maintained cardiac pumping in anoxic crucian carp. *Science* 306: 77, 2004.
69. **Stecyk JAW, Stensløkken KO, Nilsson GE, Farrell AP.** Adenosinergic cardiovascular control in anoxia-tolerant vertebrates during prolonged oxygen deprivation. *Comp Biochem Physiol A* 147: 961–973, 2007.
70. **Stecyk JAW, Paajanen V, Farrell AP, Vornanen M.** Effect of temperature and prolonged anoxia exposure on electrophysiological properties of the turtle (*Trachemys scripta*) heart. *Am J Physiol Regul Integr Comp Physiol* 293: R421–R437, 2007.
71. **Stecyk JAW, Galli GL, Shiels HA, Farrell AP.** Cardiac survival in anoxia-tolerant vertebrates: An electrophysiological perspective. *Comp Biochem Physiol C* 148: 339–354, 2008.
72. **Storey KB.** Metabolic adaptations supporting anoxia tolerance in reptiles: Recent advances. *Comp Biochem Physiol B* 113: 23–35, 1996.
73. **Ultsch GR.** The ecology of overwintering among turtles: where turtles overwinter and its consequences. *Biol Rev Camb Philos Soc* 81: 339–367, 2006.

74. **Vornanen M, Shiels HA, Farrell AP.** Plasticity of excitation-contraction coupling in fish cardiac myocytes. *Comp Biochem Physiol A* 132: 827–846, 2002.
75. **Wasser JS, Freund EV, Gonzalez LA, Jackson DC.** Force and acid-base state of turtle cardiac tissue exposed to combined anoxia and acidosis. *Am J Physiol Regul Integr Comp Physiol* 259: R15–R20, 1990.
76. **Wasser JS, Inman KC, Arendt EA, Lawler RG, Jackson DC.** ^{31}P-NMR measurements of pH_i and high-energy phosphates in isolated turtle hearts during anoxia and acidosis. *Am J Physiol Regul Integr Comp Physiol* 259: R521–R530, 1990.
77. **Wasser JS, Meinertz EA, Chang SY, Lawler RG, Jackson DC.** Metabolic and cardiodynamic responses of isolated turtle hearts to ischemia and reperfusion. *Am J Physiol Regul Integr Comp Physiol* 262: R437–R443, 1992.
78. **Wasser JS, Vogel L, Guthrie SS, Stolowich N, Chari M.** ^{31}P-NMR determinations of cytostolic phosphodiesters in turtle hearts. *Comp Biochem Physiol A* 118: 1193–1200, 1997.
79. **Wasser JS, Guthrie SS, Chari M.** In vitro tolerance to anoxia and ischemia in isolated hearts from hypoxia sensitive and hypoxia tolerant turtles. *Comp Biochem Physiol A* 118: 1359–1370, 1997.
80. **Wemmer D, Wade-Jardetzky N, Robin E, Jardetzky O.** Changes in the phosphorous metabolism of a diving turtle observed by ^{31}P-NMR. *Biochim Biophys Acta* 720: 281–287, 1982.
81. **Wu F, Zhang EY, Zhang J, Bache DA, Beard RJ.** Phosphate metabolite concentrations and ATP hydrolysis potential in normal and ischemic hearts. *J Physiol* 586: 4193–4208, 2008.
82. **Vaughn-Jones RD, Spitzer KW, Swietach P.** Intracellular pH regulation in heart. *J Mol Cell Cardiol* 46: 318–331, 2009.
83. **Yee HP, Jackson DC.** The effects of different types of acidosis and extracellular calcium on the mechanical activity of turtle atria. *J Comp Physiol [B]* 154: 385–391, 1984.
84. **Zhou L, Yu X, Cabrera ME, Stanley WC.** Role of cellular compartmentation in the metabolic response to stress: mechanistic insights from computational models. *Ann N Y Acad Sci* 1080: 120–139, 2006.

Supporting Material

Correlation of cardiac performance with cellular energetic components in the oxygen-deprived turtle heart

Jonathan A. W. Stecyk, Christian Bock, Johannes Overgaard, Tobias Wang, Anthony P. Farrell & Hans-O. Pörtner

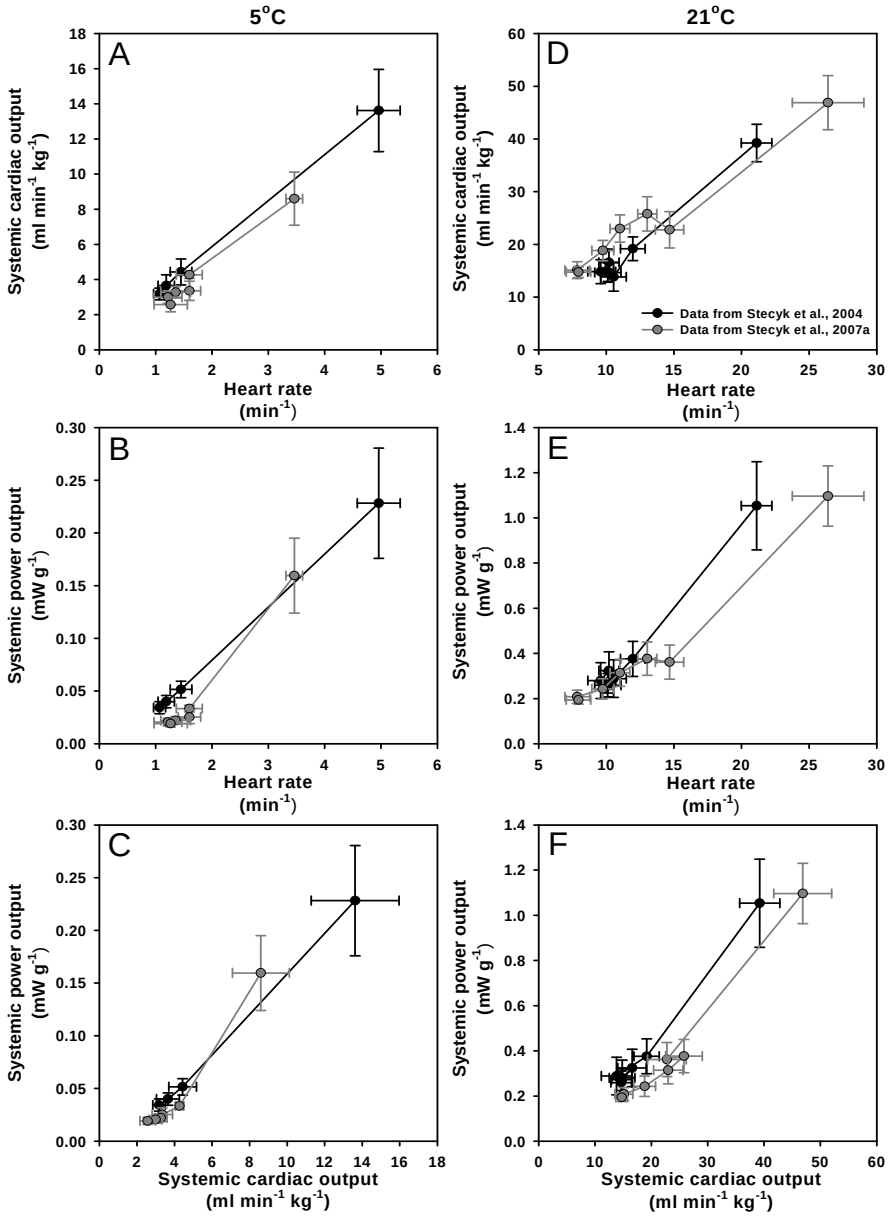

Fig. S1. Relationship between (A, D) heart rate and systemic cardiac output, (B, E) heart rate and systemic cardiac power output and (C, F) systemic cardiac output and systemic cardiac power output in 21ºC- and 5ºC-acclimated turtles during anoxia exposure (6 h at 21ºC and 12 – 14 days at 5ºC). Values are means ± S.E.M.; *N*= 5-8. Data are adapted from Refs. S1 and S2. Please note the different scaling of y- and x-axis between temperature acclimation groups.

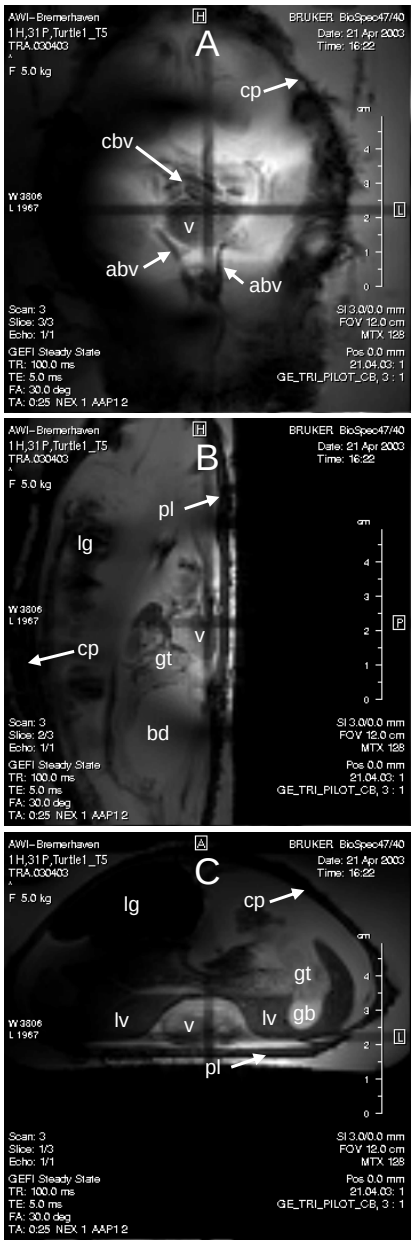

Fig. S2. Representative (A) coronal, (B) sagittal and (C) transverse scout images of a turtle within the MR magnet. The cross-hairs (darkened lines) indicate the center of the magnet, within which lies the turtle heart. Morphological features: abv, abdominal vein; bd, bladder; cbv, central blood vessels; cp, carapace; gb, gall blader; gt, gut; lg, lung; lv, liver; pl, plastron; v, ventricle.

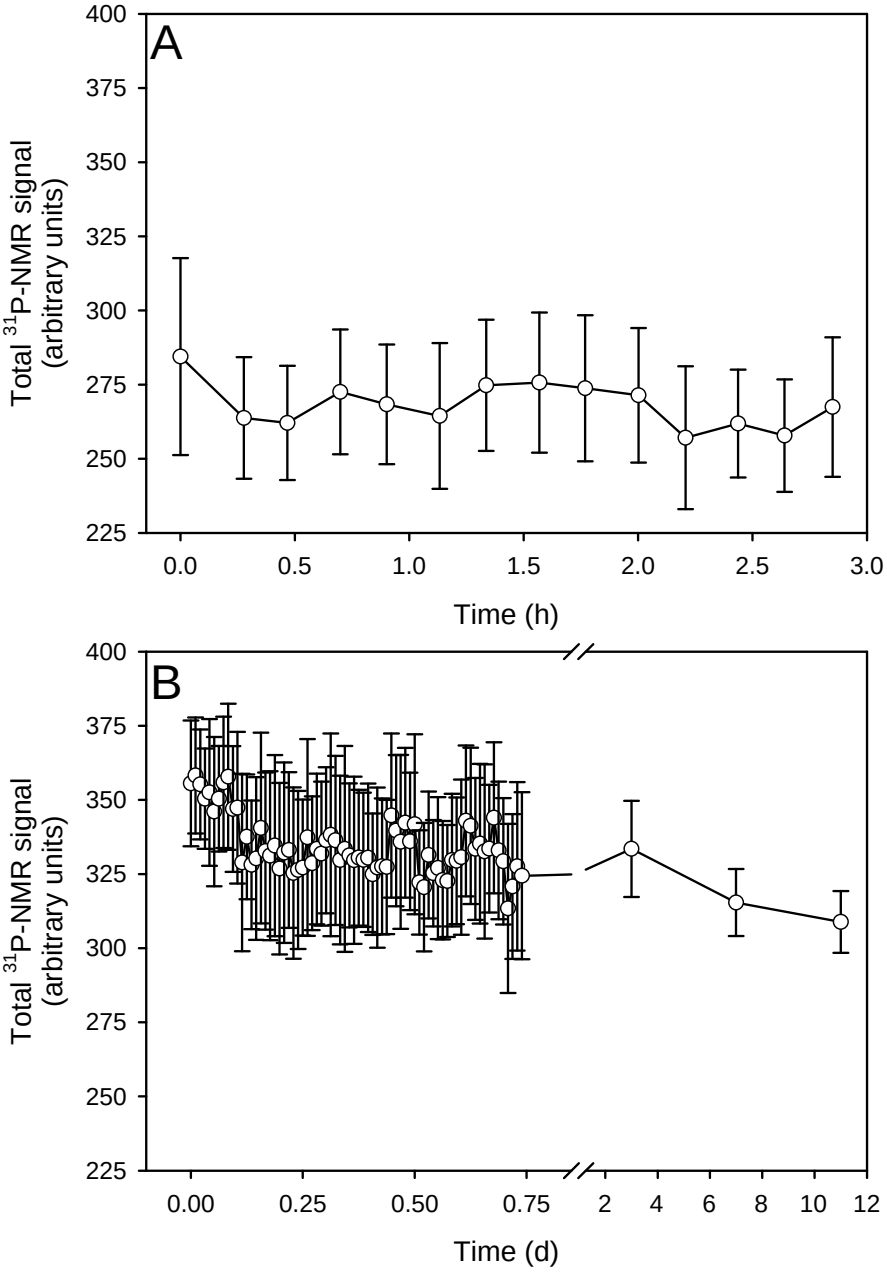

Fig. S3. Total ^{31}P-NMR signal of (A) 21ºC-acclimated and (B) 5ºC-acclimated turtle hearts during prolonged anoxia exposure. Note the different time-scale between temperature acclimation groups. Values are means ± S.E.M.; *N*= 5-7.

Supporting References

S1. **Stecyk JAW, Overgaard J, Farrell AP and Wang T.** α-Adrenergic regulation of systemic peripheral resistance and blood flow distribution in the turtle (*Trachemys scripta*) during anoxic submergence at 5°C and 21°C. *J Exp Biol* 207: 269-283, 2004.

S2. **Stecyk JAW, Stensløkken K-O, Nilsson GE, Farrell AP.** Adenosinergic cardiovascular control in anoxia-tolerant vertebrates during prolonged oxygen deprivation. *Comp Biochem Physiol A* 147: 961-973, 2007.